



A comparison of Finite difference schemes to Finite volume scheme for axially symmetric 2D heat equation

Ramesh Chandra Timsina^{*1}

¹Department of Mathematics, Patan Multiple Campus, Tribhuvan University,
Kathmandu, Nepal
timsinaramesh72@yahoo.com

Received: 5 March, 2024 Accepted: 12 May, 2024 Published Online: 30 June, 2024

Abstract

In this work, we compare finite difference schemes to finite volume scheme for axially symmetric 2D heat equation with Dirichlet and Neumann boundary conditions. Using cylindrical coordinate geometry, we describe a mathematical model of axially symmetric heat conduction for a stationary, homogeneous isotropic solid with uniform thermal conductivity in a hollow cylinder with an exact solution in a particular case. We obtain the numerical solution of the PDE adapting finite difference and finite volume discretization techniques. Compared to the exact solution, we explore that the numerical schemes are the sufficient tools for the solution of linear or nonlinear PDE with prescribed boundary conditions. Furthermore, the numerical solution discrepancies in the results obtained from Explicit, Implicit and Crank-Nicolson schemes in Finite Difference Method (FDM) are extremely close to the exact solution in the case of Dirichlet boundary condition. The solution from Explicit scheme is slightly far from the exact solution and the solutions from Implicit and Crank-Nicolson schemes are extremely close to the exact solution in the case of Neumann boundary condition. Likewise, the numerical solutions obtained in Finite volume method (FVM) are extremely close to the exact solution in the case of Dirichlet boundary condition and slightly away from exact solution in the case of Neumann boundary condition.

Keywords: Finite difference scheme, Finite volume scheme, Axially Symmetric, Heat conduction, Boundary conditions.

AMS(MOS) Subject Classification: 35K05 58J35.

1 Introduction

Partial differential equations are the most applied model to describe the physical phenomena in real-world problems. Many physical, chemical, biological, and environmental phenomena of the real world can govern a mathematical problem or a mathematical model [1]. Researchers are trying to describe these phenomena by imposing various factors to govern the situations in the form of Partial Differential Equation (PDE) [2]. They also seek the components involved in the areas of applications, mathematical description, formulation, and computing approaches. Numerous models can be developed by capturing the scenario of the real phases; however, applied aspects of the model are only possible with its mathematical and computing aspects. Only mathematical aspects of the numerical PDE can be developed, but it can only give results with applications and computing.

Numerical methods based on computing are the major tool for solving large scale linear and nonlinear problems. Advancing in computer technology, parallel computing, numerical discretization etc. are the potential growing factors in the computational regime. In recent years much effort has been devoted to develop computational schemes for numerical approaches to solve physical problems govern by PDE. In computational world, finite difference, finite element, finite volume, spectral methods, collocation methods are the most effective and widely used numerical techniques [2][3][4].

The calculus of finite differences is the primary features of finite difference schemes. In which the derivatives terms of the PDEs are expressed in the form of difference equations. By this mean, the continuous problem is changed into a discrete problem with a finite number of equations. Those equations give the relationships between the dependent variables to the prescribed interconnected points with boundaries in the space in which the position vector can interpolate with given located time. Furthermore, each derivative term of the PDE is approximate with Taylor's series expansion and then the set of finite difference equation are solved numerically by computer and depict the value of dependent variables on the corresponding grid points. On the other side in the finite volume method, the governing PDE is satisfied over finite-sized control volume. It is based on integral formulation of the problem in terms of conservation laws. In finite volume method, a local balance equation is written on each discretized finite-sized control volume and an integral formulation of the fluxes over the boundary(faces) is then obtained using the divergence theorem. Then the fluxes are discretized in terms of the discrete unknowns. In both schemes, the boundary grid points of the computational domain can be prescribed as direct value of the dependent variables called Dirichlet boundary condition or by the value of gradient of the dependent variable normal to the boundary called as Neumann boundary condition. Here, in our work, we have applied different finite difference schemes and finite volume scheme for axially symmetrical 2D heat equation and compared their performance taking into account with

its exact solution for the prescribed conditions [5][6].

The main aim of this work is to present a reliable and accurate numerical approximation for the computation of axially symmetric 2D heat equation based on its particular exact solution. It also presents the potentiality of the computational approximation on the prescribed boundaries with their computational cost.

The work is organized as follows: In section 2, we present the model equation. The finite difference and finite volume discretization techniques are presented in section 3. We present the result and discussion in section 4 and in section 5 we concluded our result.

2 Mathematical Model

Using cylindrical coordinates, the axially symmetric heat conduction for a stationary, homogeneous, isotropic solid with uniform thermal conductivity in a hollow cylinder can be described by the following initial boundary value problem of partial differential equation as [7][8]:

$$\frac{\partial u}{\partial t} = D \left(\frac{1}{r} \frac{\partial}{\partial r} \left(r \frac{\partial u}{\partial r} \right) + \frac{\partial^2 u}{\partial z^2} \right) + \frac{1}{\rho c} s(t), \quad R_{in} \leq r \leq R_{out}, \quad 0 \leq z \leq Z_{top}, \quad t > 0 \quad (2.1)$$

where, $D = \frac{k}{\rho c}$ and $s(t) = \frac{1}{1+t}$, $\rho = 1, k = 1, c = 1$

If we set diffusivity $D = 1$, $R_{in} = 1$, $R_{out} = 2$, $Z_{top} = \pi$, initial condition $u(r, z, 0) = \ln(r) \sin(z)$ and boundary conditions $u(R_{in}, z, t) = 0$, $u(R_{out}, z, t) = \ln 2 e^{-t} \sin z$, $u(r, 0, t) = 0$, $u(r, \pi, t) = 0$, we can get the exact solution as :

$$u(r, z, t) = \ln(r) e^{-t} \sin(z)$$

Now the prescribed initial and boundary conditions are:

Initial condition

$$u(r, z, 0) = \log(r) \sin(z)$$

corresponding Dirichlet boundary conditions

$$u(R_{in}, z, t) = e^{-t} \log(R_{in}) \sin(z) + s(r, z, t)$$

$$u(R_{out}, z, t) = e^{-t} \log(R_{out}) \sin(z) + s(r, z, t)$$

$$u(r, Z_{bot}, t) = e^{-t} \log(r) \sin(z) + s(r, z, t)$$

$$u(r, Z_{top}, z, t) = e^{-t} \log(r) \sin(z) + s(r, z, t)$$

and Neumann boundary conditions

$$\frac{\partial}{\partial r} (u(R_{in}, z, t)) = \frac{1}{R_{in}} e^{-t} \sin(z)$$

$$\frac{\partial}{\partial r} (u(R_{out}, z, t)) = \frac{1}{R_{out}} e^{-t} \sin(z)$$

$$u(r, Z_{bot}, t) = e^{-t} \log(r) \sin(z) + s(r, z, t)$$

$$\frac{\partial}{\partial z} (u(r, Z_{top}, t)) = e^{-t} \log(r) \cos(z)$$

3 Numerical Method

To solve equation 2.1 numerically, we use finite difference schemes and finite volume scheme and compare the result with the prescribed initial and boundary conditions. Since we set particular conditions for the exact solution, we compare the results obtain the above numerical results to the exact solution. For the numerical procedure, firstly we construct the geometry of axially symmetrical model and make a nodal arrangement in a definite domain [5][3] .

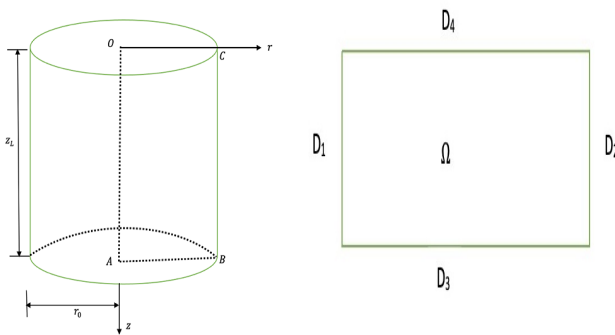


Figure 1: Cylindrical Body(right), Domain with boundary(left)

3.1 Finite Difference Discretization

We set up a two dimensional (r, z) uniform grid for an axi-symmetric problem in the cylinder geometry by subdividing the radial length $[R_{in}, R_{out}]$ into M_r subintervals of width $\Delta r = \frac{R_{out} - R_{in}}{M_r}$ and the height $[0, Z_{top}]$ into M_z subintervals of width $\Delta z = \frac{Z_{top}}{M_z}$. We construct a

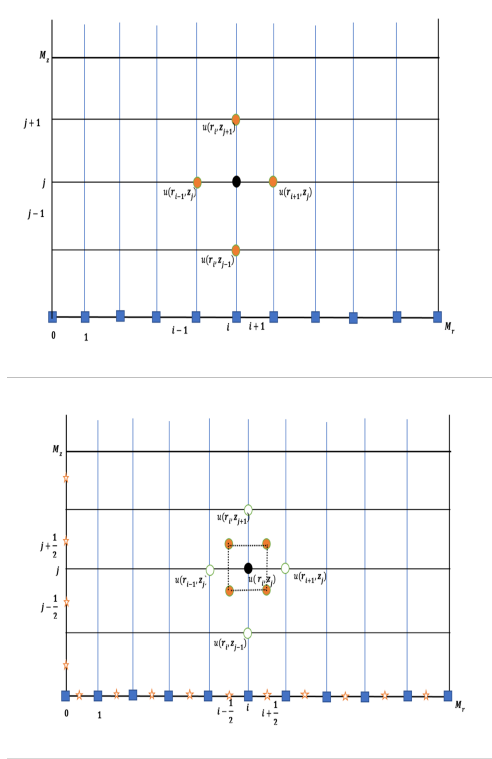


Figure 2: Mesh in FDM and FVM

grid (r_i, z_j, t_n) with $r_i = i\Delta r, i = 0, 1, 2, \dots, M_r, z_j = j\Delta z, j = 0, 1, 2, \dots, M_z,$ and $t_n = n\Delta t, n = 1, 2, \dots, N$. Let $u_{i,j}^n$ denote $u(r_i, z_j, t_n)$. The partial differential equation (2.1) can be approximated using forward difference in time and central difference in space on radial and axial direction as[9]

$$\begin{aligned} \frac{\partial u}{\partial t} \Big|_{(r_i, z_j, t_n)} &\approx \frac{u_{i,j}^{n+1} - u_{i,j}^n}{\Delta t}, & \frac{\partial u}{\partial r} \Big|_{(r_i, z_j, t_n)} &\approx \frac{u_{i+1,j}^n - u_{i-1,j}^n}{\Delta r} \\ \frac{\partial^2 u}{\partial r^2} \Big|_{(r_i, z_j, t_n)} &\approx \frac{u_{i-1,j}^n - 2u_{i,j}^n + u_{i+1,j}^n}{\Delta r^2} & \frac{\partial^2 u}{\partial z^2} \Big|_{(r_i, z_j, t_n)} &\approx \frac{u_{i,j-1}^n - 2u_{i,j}^n + u_{i,j+1}^n}{\Delta z^2}. \end{aligned} \tag{3.1}$$

Again approximating equation (2.1) using backward difference in time and central difference in space on radial and axial direction as

$$\begin{aligned} \frac{\partial u}{\partial t} \Big|_{(r_i, z_j, t_{n+1})} &\approx \frac{u_{i,j}^{n+1} - u_{i,j}^n}{\Delta t}, & \frac{\partial u}{\partial r} \Big|_{(r_i, z_j, t_{n+1})} &\approx \frac{u_{i+1,j}^{n+1} - u_{i-1,j}^{n+1}}{\Delta r} \\ \frac{\partial^2 u}{\partial r^2} \Big|_{(r_i, z_j, t_{n+1})} &\approx \frac{u_{i-1,j}^{n+1} - 2u_{i,j}^{n+1} + u_{i+1,j}^{n+1}}{\Delta r^2} & \frac{\partial^2 u}{\partial z^2} \Big|_{(r_i, z_j, t_{n+1})} &\approx \frac{u_{i,j-1}^{n+1} - 2u_{i,j}^{n+1} + u_{i,j+1}^{n+1}}{\Delta z^2}. \end{aligned} \tag{3.2}$$

Similarly approximating equation(2.1) using Crank-Nicolson scheme on radial and axial direction as

$$\begin{aligned} & \frac{1}{\Delta t} \left[u_{i,j}^{n+1} - u_{i,j}^n \right] = \\ & \theta \left[D \left\{ \frac{u_{i-1,j}^{n+1} - 2u_{i,j}^{n+1} + u_{i+1,j}^{n+1}}{(\Delta r)^2} + \frac{1}{r_i} \frac{u_{i+1,j}^{n+1} - u_{i-1,j}^{n+1}}{(2\Delta r)} + \frac{u_{i,j-1}^{n+1} - 2u_{i,j}^{n+1} + u_{i,j+1}^{n+1}}{(\Delta z)^2} \right\} + s(r_i, z_j, t^n) \right] \\ & + (1 - \theta) \left[D \left\{ \frac{u_{i-1,j}^n - 2u_{i,j}^n + u_{i+1,j}^n}{(\Delta r)^2} + \frac{1}{r_i} \frac{u_{i+1,j}^n - u_{i-1,j}^n}{(2\Delta r)} + \frac{u_{i,j-1}^n - 2u_{i,j}^n + u_{i,j+1}^n}{(\Delta z)^2} \right\} + s(r_i, z_j, t^{n+1}) \right] \\ & \qquad \qquad \qquad i = 1, 2 \dots, M_r - 1, \quad j = 1, 2 \dots, M_z - 1 \end{aligned} \quad (3.3)$$

where, $0 \leq \theta \leq 1$ be a weighted average of the derivative $\frac{\partial^2 u}{\partial r^2}$, $\frac{\partial^2 u}{\partial z^2}$, and $\frac{\partial u}{\partial r}$ at two time label t_n and t_{n+1} .

We collect the unknowns on the left hand side, then equation (3.3) becomes

$$\begin{aligned} & u_{i,j}^{n+1} - \theta \left[F_r \left(u_{i-1,j}^{n+1} - 2u_{i,j}^{n+1} + u_{i+1,j}^{n+1} \right) + \frac{F_{r_1}}{r_i} \left(u_{i+1,j}^{n+1} - u_{i-1,j}^{n+1} \right) + F_z \left(u_{i,j-1}^{n+1} - 2u_{i,j}^{n+1} + u_{i,j+1}^{n+1} \right) \right] \\ & = (1 - \theta) \left[F_r \left(u_{i-1,j}^n - 2u_{i,j}^n + u_{i+1,j}^n \right) + \frac{F_{r_1}}{r_i} \left(u_{i+1,j}^n - u_{i-1,j}^n \right) + F_z \left(u_{i,j-1}^n - 2u_{i,j}^n + u_{i,j+1}^n \right) + \Delta t s(r_i, z_j, t^n) \right] \\ & \qquad \qquad \qquad + \Delta t \theta s(r_i, z_j, t^{n+1}) + u_{i,j}^n \quad i = 1, 2 \dots, M_r - 1, \quad j = 1, 2 \dots, M_z - 1 \end{aligned} \quad (3.4)$$

$$\text{Where, } F_r = \frac{D\Delta t}{(\Delta r)^2}, \quad F_{r_1} = \frac{D\Delta t}{(\Delta r)} \quad \text{and} \quad F_z = \frac{D\Delta t}{(\Delta z)^2}$$

In numerical solution of equation (3.4), it is coupled at the new time label $n + 1$. That is, we must solve a system of (linear) algebraic equations, which we will write as $CX = D$, where C is the coefficient matrix, X is the vector of unknowns, D is the right hand-side [10][11].

To solve the above system of linear equations, we have a matrix system $CX = D$, where the solution vector X must have one index. For this, we need a numbering of the unknowns with one index, not two as used in the mesh. We introduce a mapping $position(i, j) = u(i, j)$ from a mesh point with indices (i, j) to the corresponding unknown q in the equation system.

$$q = u(i, j) = j(M_r + 1) + i, \quad \text{for } i = 0, 1, 2, \dots, M_r, \quad j = 0, 1, 2, \dots, M_z,$$

With this mapping, we number the points along the radial direction starting with $z = 0$ and then filled one mesh line at a time. In another way

$$q = m(i, j) = i(M_z + 1) + j, \quad \text{for } i = 0, 1, 2, \dots, M_r, \quad j = 0, 1, 2, \dots, M_z.$$

with $r = 0$ and then filled one mesh line at a time. From this we can get the general feature of the coefficient matrix obtained from the discretized equation (3.4).

Now $C_{q,p}$ be the value of element (q,p) in the coefficient matrix C , where q and p are the numbering of the unknowns in the equation system. The then $C_{q,q} = 1$ for $q = p$ corresponding to the all known boundary values. q be $m(i,j)$, i.e., the single index corresponding to the mesh point (i,j) . Then, for interior mesh along with boundary, we have

$$\begin{aligned}
 C_{pos(i,j),pos(i,j)} &= C_{q,q} = 1 + \theta(2F_r + 2F_z). \\
 C_{q,pos(i-1,j)} &= A_{q,q-1} = \theta(-F_r + \frac{F_{r1}}{r_i}). \\
 C_{q,pos(i+1,j)} &= C_{q,q+1} = \theta(-F_r - \frac{F_{r1}}{r_i}). \\
 C_{q,pos(i,j-1)} &= C_{q,q-(M_z+1)} = -\theta F_z. \\
 C_{q,pos(i,j+1)} &= C_{q,q+(M_z+1)} = -\theta F_z.
 \end{aligned}$$

Right hand side of in vector with d_q in equations (3.4)

$$\begin{aligned}
 j = 0, \text{ for } i = 0, \dots, m_r \quad d_q &= exact(r_i, z_{bot}(= 0), t) = 0. \\
 j = M_z, \text{ for } i = 0, \dots, m_r \quad d_q &= exact(r_i, z_{top}(= \pi), t) = 0. \\
 i = 0, \text{ for } j = 0, \dots, m_z \quad d_q &= exact(r_{in}(= 1), z_j, t) = 0. \\
 i = 0, \text{ for } j = 0, \dots, m_z \quad d_q &= exact(r_{out}(= 2), z_j, t) = e^{-t} \ln(2) \sin(z_j).
 \end{aligned}$$

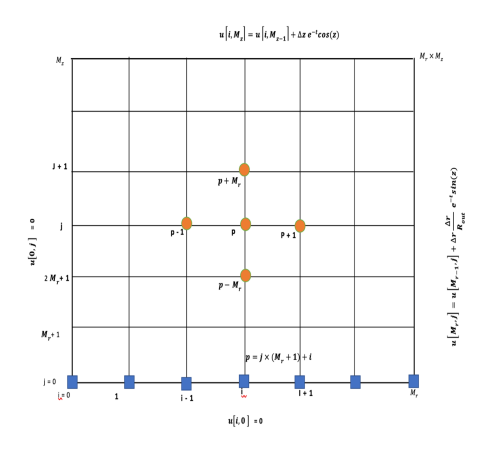


Figure 3: Discretization of 2D mesh

3.2 Finite Volume Discretization

Axi-Symmetric 2D mesh in (r, z) coordinates: We set up a two dimensional (r, z) uniform mesh with

$$\Delta r = \frac{R_{out} - R_{in}}{M_r}, \quad \Delta z = \frac{Z_{top} - Z_{bottom}}{M_z}.$$

and assign one node (r_i, z_j) to each control volume $V_{i,j}$. For nodes r_i and z_j

$$\begin{aligned} r_0 &= R_{in}, r_i = r_0 + (i - \frac{1}{2})\Delta r, i = 1, \dots, M_r, r_{M_r+1} = R_{out} \\ z_0 &= 0, z_j = (j - \frac{1}{2})\Delta z, j = 1, \dots, M_z, z_{M_z+1} = Z_{top}. \end{aligned}$$

For faces $r_{i-\frac{1}{2}}, z_{j-\frac{1}{2}}$

$$r_{i-\frac{1}{2}} = \frac{1}{2}(r_{i-1} + r_i), i = 2, 3, \dots, M_{r+1}, z_{j-\frac{1}{2}} = \frac{1}{2}(z_{j-1} + z_j), j = 2, 3, \dots, M_{z+1}.$$

The volume $V_{i,j}$ is given by

$$V_{i,j} = 2\pi \int_{r_{i-\frac{1}{2}}}^{r_{i+\frac{1}{2}}} \int_{z_{j-\frac{1}{2}}}^{z_{j+\frac{1}{2}}} dz r dr = \pi(r_{i+\frac{1}{2}}^2 - r_{i-\frac{1}{2}}^2)\Delta z_j.$$

Area of radial ($A_{i-\frac{1}{2},j}$) and axial ($A_{i,j-\frac{1}{2}}$) faces are:

$$\begin{aligned} A_{i-\frac{1}{2},j} &= 2\pi \int_{z_{j-\frac{1}{2}}}^{z_{j+\frac{1}{2}}} r_{i-\frac{1}{2}} dz = 2\pi r_{i-\frac{1}{2}} \Delta z_j \\ A_{i,j-\frac{1}{2}} &= 2\pi \int_{r_{i-\frac{1}{2}}}^{r_{i+\frac{1}{2}}} r dr = \pi(r_{i+\frac{1}{2}}^2 - r_{i-\frac{1}{2}}^2). \end{aligned} \quad (3.5)$$

3.3 Finite Volume Algorithm(explicit in time)

:

First, we write the PDE i.e. equation (2.1) in divergence form :

$$\frac{\partial u}{\partial t} = \nabla \cdot F + S(t). \quad (3.6)$$

where the heat flux F is given by

$$F = (K \frac{\partial u}{\partial r}, K \frac{\partial u}{\partial t}). \quad (3.7)$$

Let $T > 0$ be the maximum time of interest, $\{t_0, \dots, t_{N_{max}}\}$ be a partition of $[0, T]$, and $\Delta t_n = t_{n+1} - t_n$ the time step size.

Integrating equation (3.6) over the control volume $V_{i,j}$ and time interval $[t_n, t_n + \Delta t_n]$, we obtain

$$\int_{t_n}^{t_n+\Delta t_n} \frac{\partial}{\partial t} \int_{V_{i,j}} u dV dt = \int_{t_n}^{t_n+\Delta t_n} \frac{\partial}{\partial t} \int_{\partial V_{i,j}} F \cdot n dA dt + \int_{t_n}^{t_n+\Delta t_n} \int_{\partial V_{i,j}} S dv dt. \quad (3.8)$$

Define $U_{i,j} \approx u(r_i, z_j, t_n)$

as the mean value over the control volume $V_{i,j}$

$$U_{i,j}^n = \frac{1}{V_{i,j}} \int_{V_{i,j}} u(r, z, t_n) dV. \quad (3.9)$$

Also introduce the numerical flux as mean value over area and time of $F_u(r, z, t)$. Then the flux integrals in equation (3.8) can be computed by $\sum_{faces}(Area \times Flux)$, the sum of the flow rates across all the faces of the control volume $V_{i,j}$, where the flow rates across the faces are expressed as

$$(AF)_{i-\frac{1}{2},j} = \frac{1}{\Delta t_n} \int_{t_n}^{t_n+\Delta t_n} \int_{A_{i-\frac{1}{2},j}} F(r, z, t) n dA dt \quad (Radial). \quad (3.10)$$

$$(AF)_{i,j-\frac{1}{2}} = \frac{1}{\Delta t_n} \int_{t_n}^{t_n+\Delta t_n} \int_{A_{i,j-\frac{1}{2}}} F(r, z, t) n dA dt \quad (Axial). \quad (3.11)$$

Let $t_{n+\theta} := t_n + \theta\Delta t_n = (1 - \theta)t_n + \theta t_{n+1}$ with $0 \leq \theta \leq 1$ be some intermediate time such that $U_{i,j}^{n+\theta} \approx u(r_i, z_j, t_{n+\theta})$ etc. Then the discretization of (3.6) describes as

$$U_{i,j}^{n+1} - U_{i,j}^n = \quad (3.12)$$

$$\frac{\Delta t_n}{V_{i,j}} \left((AF)_{i-\frac{1}{2},j}^n + (AF)_{i+\frac{1}{2},j}^n + (AF)_{i,j-\frac{1}{2}}^n + (AF)_{i,j+\frac{1}{2}}^n \right) + dt S(r_i, z_j, t).$$

Now the flow rates at the faces are given by:

$$(AF)_{i-\frac{1}{2},j}^n = -A_{i-\frac{1}{2},j} D \left(\frac{U_{i,j} - U_{i-1,j}}{r_i - r_{i-1}} \right). \quad (3.13)$$

$$(AF)_{i+\frac{1}{2},j}^n = A_{i+\frac{1}{2},j} D \left(\frac{U_{i+1,j} - U_{i,j}}{r_{i+1} - r_i} \right). \quad (3.14)$$

$$(AF)_{i,j-\frac{1}{2}}^n = -A_{i,j-\frac{1}{2}} D \left(\frac{U_{i,j} - U_{i,j-1}}{z_j - z_{j-1}} \right). \quad (3.15)$$

$$(AF)_{i,j+\frac{1}{2}}^n = A_{i,j+\frac{1}{2}} D \left(\frac{U_{i,j+1} - U_{i,j}}{z_{j+1} - z_j} \right). \quad (3.16)$$

The flow rates at the faces and the corresponding boundaries are:

for $i = 2, \dots, M_{r+1}$

for $j = 1, \dots, M_{z+1}$

$$F_r = \frac{U_{i-1,j} - U_{i,j}}{R_r}. \quad (3.17)$$

for $i = 1, \dots, M_{r+1}$

for $j = 2, \dots, M_{z+1}$

$$F_z = \frac{U_{i,j-1} - U_{i,j}}{R_z}. \quad (3.18)$$

Imposing the temperature in all faces(Boundary condition)

for $j = 1, \dots, M_{z+1}$

$$(F_r)_{1,j} = \frac{-2(U_{1,j} - u(R_{in}, z, t))}{R_r}. \quad (3.19)$$

$$(F_r)_{M_{r+1},j} = \frac{2(U_{M_{r+1},j} - u(R_{out}, z, t))}{R_r}. \quad (3.20)$$

for $i = 1, \dots, M_{r+1}$

$$(F_z)_{i,1} = \frac{-2(U_{i,1} - u(r, z_{bot}, t))}{R_z}. \quad (3.21)$$

$$(F_z)_{i,M_z+1} = \frac{2(U_{i,M_z} - u(r, z_{top}, t))}{R_z}. \quad (3.22)$$

And the corresponding PDE with boundary condition is :

$$U_{i,j} = cf((F_r)_{i,j}(A_r)_{i,j} - (F_r)_{i+1,j}(A_r)_{i+1,j} + (F_z)_{i,j}(A_z)_{i,j} - (F)_{i,j+1}(A_z)_{i,j+1}) + dt S(r_i, z_j, t). \quad (3.23)$$

For $j = 1, \dots, M_{z+2}$

$$U_{0,j} = exact(R_{in}, z_j, t). \quad (3.24)$$

$$U_{M_{r+1},j} = exact(R_{out}, z_j, t). \quad (3.25)$$

For $i=1, \dots, M_{r+1}$

$$U_{i,0} = exact(r_i, z_{bot}, t). \quad (3.26)$$

$$U_{i,M_{z+1}} = exact(r_i, z_{top}, t). \quad (3.27)$$

3.4 Courant - Friedrichs - Lewy(CFL) condition

Explicit schemes are very simple and convenient from the implementation point of view. However, a computational cost is to be paid by the restriction in time size to ensure the numerical stability of the scheme [12]. There are various ways to analyze the stability of numerical methods: von Neumann analysis, M matrix method, Positive coefficient rule. We apply the later, which ensures the positivity of the scheme. We rewrite the equation (3.12) in the form

$$U_{i,j}^{n+1} = \alpha_{i,j} U_{i-1,j}^n + \alpha_{i+1,j} U_{i+1,j}^n + (1 - \gamma_{i,j}) U_{i,j}^n + \beta_{i,j} U_{i,j-1}^n + \beta_{i,j+1} U_{i,j+1}^n \quad (3.28)$$

for $n = 1, 2, \dots, N_{max}$, $i = 1, 2, \dots, M_r$ $j = 1, 2, \dots, M_z$, where

$$\alpha_{i,j} = \frac{\Delta t_n}{V_{i,j}} \frac{A_{i-\frac{1}{2},j}}{(r_i - r_{i-1})} D, \text{ for } i = 1, 2, \dots, M_r + 1, j = 1, 2, \dots, M_z. \quad (3.29)$$

$$\beta_{i,j} = \frac{\Delta t_n}{V_{i,j}} \frac{A_{i,j-\frac{1}{2}}}{(z_j - z_{j-1})} D, \text{ for } i = 1, 2, \dots, M_r, j = 1, 2, \dots, M_z + 1. \quad (3.30)$$

$$\gamma_{i,j} = \alpha_{i,j} + \alpha_{i+1,j} + \beta_{i,j} + \beta_{i,j+1} \text{ for } i = 1, 2, \dots, M_r, j = 1, 2, \dots, M_z. \quad (3.31)$$

to ensure positive coefficient in equation (3.28), we need $\gamma_{i,j} < 1$, which requires

$$\Delta t < \frac{0.5}{\frac{D}{(\Delta r)^2} + \frac{D}{(\Delta z)^2}} \leq \frac{\min\{(\Delta r)^2, (\Delta z)^2\}}{4D}. \quad (3.32)$$

And stability analysis of the equation (3.4) is analyzed at [13].

4 Results and Discussion

The numerical algorithm developed in section 3.1 and 3.2 are written in python and ran on a laptop with 2.8 GHz Quad-Core Intel Core i7 processor[14]. The numerical solution of the equation (2.1) is carried out using forward difference (Explicit), backward difference (Implicit), Crank-Nicolson and finite volume (Explicit in time) methods with imposing Dirichlet and Neumann Boundary conditions. Since the exact solution for the particular case is calculated and we compare the numerical solutions. Figure 4 (left) depicts the longitudinal temperature profile with dirichlet boundary condition for the three finite difference schemes. From figure 4 (left) we can state directly that there is no significant difference between the schemes. Figure 4 (right) illustrate the numerical results of longitudinal temperature profile with imposing the Neumann boundary condition. It shows that the explicit scheme has little contrast in exact solution. Also figure 5 left and (right) depict the radial temperature profile with both boundary condition which explore the same result as figure 4 and figure 6 and 7 describe that the numerical solution obtained from finite volume method are close to the exact solution in imposing Dirichlet boundary condition and slightly away from exact solution in Neumann boundary condition. Table 1 explore the CPU time(s) execute time and the corresponding error of the eight different schemes in the case of axially symmetric heat conduction equation.

Table 1: Comparison with CPU time and Error

Schemes	Boundary condition	CPU time(s)	Error
Explicit	Dirichlet	29.4286830	.00035762189
Implicit	Dirichlet	29.4286830	.0003280250
CN	Dirichlet	29.4286830	.00066223219
Implicit	Neumann	29.484686374	.0047332550
Implicit	Neumann	29.484686374	.00467332250
CN	Neumann	29.484686374	.004955038
Finite Volume	Neumann	16.18792581	.0246761
Finite Volume	Dirichlet	16.3679363	.0001212

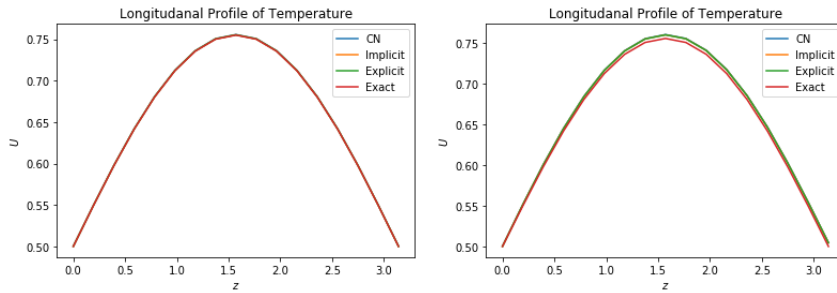


Figure 4: Longitudinal temperature profile with dirichlet boundary (left) and Neumann boundary condition in (right)

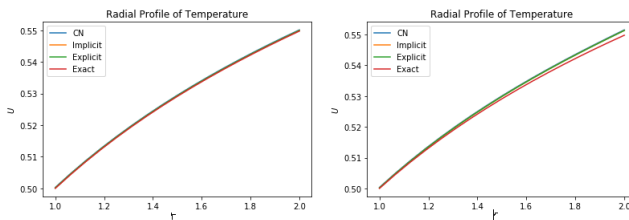


Figure 5: Radial temperature profile with dirichlet boundary (left) and Neumann boundary condition in (right)

5 Conclusion

In this work, we explored the finite difference schemes and finite volume scheme to find the numerical solution of heat conduction equation (a PDE) in axially symmetric cylindrical coordinate system. Two boundary conditions Dirichlet and Neumann were imposed in the PDE correspondingly. The PDE has also an exact solution for a certain condition. With based on the exact solution the different numerical schemes are compared and their performance are explored. From the result obtained above we can conclude that the numerical schemes are the sufficient tools for obtaining the solution of linear and non linear PDE having exact solution or not. We also observed that the consistency, uniqueness and the stability of the numerical techniques also depends on the imposing boundary condition and the physical condition for the problem. It is shown that the reliability and the accuracy of the schemes depends on the prescribed boundary conditions of the problems. From table 1 depicted above, we can observed that Finite volume method is more appropriate to get the numerical solution for the type of parabolic equation we have taken.

Data Availability

The data used for supporting the findings of this study are included within the article.

Conflicts of Interest

The author declares that there is no conflict of interest.

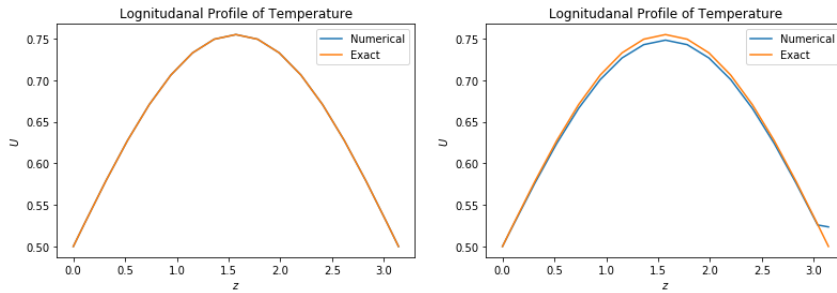


Figure 6: Longitudinal temperature profile with Dirichlet boundary (left) and Neumann boundary condition in (right)

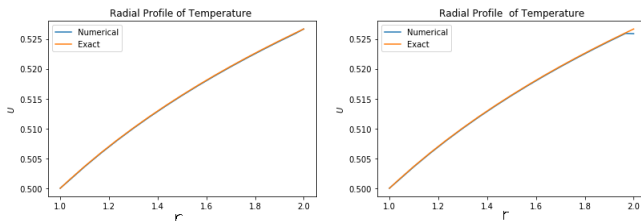


Figure 7: Radial temperature profile with Dirichlet boundary (left) and Neumann boundary condition in (right)

References

- [1] L. C. Evans, "Partial Differential equations" *Am. Math. Soc., Providence* 2000.
- [2] W. Cheney, D. Kincaid, Numerical Mathematics and Computing, 7th ed., *Brooks/Cole Publishing Company*, 2013.
- [3] H. K. Versteeg, and W. Malalasekera, An introduction to computational fluid dynamics The finite volume method, *Pearson Educational Limited, second Edition*, 2007.
- [4] T.N. Narasimhan, and P.A. Witherspoon, An Integrated Finite Difference Method for Analyzing Fluid Flow in Porous Media, *Water Resour. Res.*, Vol. 12, pp 57-64, 1976.
- [5] J.W. Thomas, Numerical partial differential equations: Finite difference methods, Text in Applied Mathematics, *Springer*, 2010.
- [6] A. Adamowicz, Axisymmetric FE Model to Analysis of Thermal Stress in a Break Disk, *Journal of Theoretical and Applied Mechanics*, 53, 2, pp. 357-370, Warsaw 2015.
- [7] F.P. Incropera, D.P. Dewitt, T.L. Bergman, A.S. Lavine, Introduction to heat transfer. 6th ed *New York: Wiley*, 2011.
- [8] E. Krezig, Advanced engineering mathematics, 10th ed. *New York: John Wiley and Sons*; 2010.

- [9] R. C. Timsina and K. N. Uprety, Comparison of finite difference scheme for fluid flow in unsaturated porous medium (soil), *The Nepali Mathematical Sciences Report*, Vol. 39, No. 1, : 22-35, 2022.
- [10] V. Thomée , From finite differences to finite elements: a short history of numerical analysis of partial differential equations. *J Comp Appl Math*; 128: 1–54, 2001.
- [11] S.V. Patankar, Numerical heat transfer and fluid flow. Washington: *Hemisphere*, 1980.
- [12] R. Courant, K.O. Friedrichs, H. Lewy, Über die partiellen Differenzgleichungen der Mathematischen *Physik. Math. Ann.* 1928;100:32–74. English translation, with commentaries by Lax PB, Widlund OB, Parter, SV, in *IBM J Res Develop* 11, 1967.
- [13] R. C. Timsina, H. Khanal, and K. N. Uprety, An explicit stabilized Runge-Kutta-Legendre super time -stepping scheme for the Richards equation, *Mathematical problems in Engineering*, vol-2021, 1–11, 2021.
- [14] H. P. Langtangen, Solving nonlinear ODE and PDE problems, *Center for Biomedical Computing, Simula Research Laboratory, 2 Department of Informatics, University of Oslo*, 2016.